Salwa Akl

بسم اللّه الرحمن الرحيم

مركز الشبكات وتكنولوجيا المعلومات

قسم التوثيق الإلكتروني

Salwa Akl

جامعة عين شمس

التوثيق الإلكتروني والميكروفيلم

قسم

نقسم باللّه العظيم أن المادة التي تم توثيقها وتسجيلها

علي هذه الأقراص المدمجة قد أعدت دون أية تغيرات

Salwa Akl

بعض الوثائق الأصلية تالفة
وبالرسالة صفحات لم ترد بالأصل

Mansoura University
Faculty of Engineering
Dep. of Electronics & Comm. Eng.

MICROWAVE FILTER DESIGN USING MULTILAYER MICROSTRIP COUPLED LINES

A thesis submitted in partial fulfillment
For the requirements of the degree of Master of Science in
Electrical Communications Engineering

By:

Eng.\ Nagi Eldesouki Mohammed

Supervisors

Prof. \ Hamdi A. Elmikati
Prof. of Comm. Faculty of Eng. Mansoura University

Dr. \ Abdo H. Elfayomi
Vice-chairman of Eng. Broadcasting Sector- ERTU

Asst. Prof. \ Maher M. Abd Elrazak
Asst. Prof.-Comm. Dept.- Faculty of Eng.- Mansoura University

2001-2002

Mansoura University
Faculty of Engineering
Dep. of Electronics & Comm. Eng.

MICROWAVE FILTER DESIGN USING MULTILAYER MICROSTRIP COUPLED LINES

**A thesis submitted in partial fulfillment
For the requirements of the degree of Master of Science in
Electrical Communications Engineering**

By:

Eng.\ Nagi Eldesouki Mohammed

Supervisors

Prof. \ Hamdi A. Elmikati
Prof. of Comm. Faculty of Eng. Mansoura University

Dr. \ Abdo H. Elfayomi
Vice-chairman of Eng. Broadcasting Sector- ERTU

Asst. Prof. \ Maher M. Abd Elrazak
Asst. Prof.-Comm. Dept.- Faculty of Eng.- Mansoura University

2001-2002

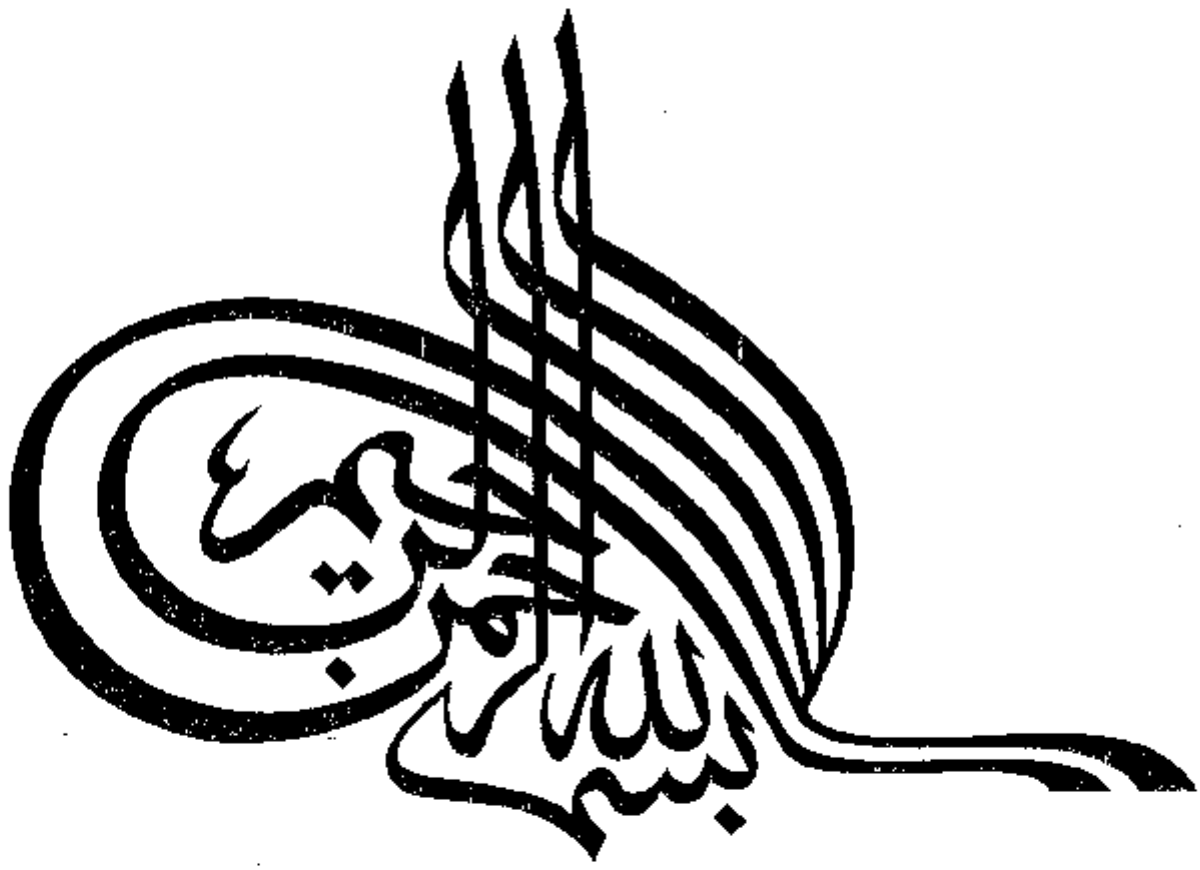
بسم الله الرحمن الرحيم

SUPERVISORS

Thesis Title:
MICROWAVE FILTER DESIGN USING MULTILAYER MICROSTRIP COUPLED LINES

Researcher Name:
Eng.\ Nagi Eldesouki Mohammed

Supervisors

No.	Name	Job	Signature
1	**Prof. \ Hamdi A. Elmikati**	**Prof. of Comm. Faculty of Eng. Mansoura University**	H. F
2	**Dr. \ Abdo H. Elfayomi**	**Vice-chairman of Eng. Broadcasting Sector- ERTU**	A. Fayom
3	**Asst. Prof. \ Maher M. Abd Elrazak**	**Asst. Prof.-Comm. Dept.- Faculty of Eng.- Mansoura University**	H. MM

DEDICATION

I dedicate this thesis to my parents who enabled me in many ways to complete this work.

AKNOWLEDGMENT

I wish to express my gratitude to my advisor Prof. Hamdi A. Elmikati, for providing me with very good material to start my work with, and for his guidance during the preparation of this thesis. I extend my sincere thankfulness to my advisor Asst. Prof. Maher M. Abd Elrazak for his cooperation, great help and guidance during the preparation of this work. I wish also to thank my advisor Dr. Abdo H. Elfayomi for discussions and his kind help and encouragement.

Many thanks to Dr. Mohammad M. Almasri and to Miss Amira R. Abdo for her help during preparing thesis draft.

I am thankful to my wife for her encouragement, support and the patience she showed throughout the preparation of this research.

ABSTRACT

In this thesis the analysis and design, of the parallel-coupled line bandpass filters (PCL-BPF) is prescnted. The filter is realized using the broadside-coupled microstrip line structure with two different layout implementations. The first layout is the PCL-BPF with open-end resonator sections, while the second layout is the PCL-BPF with gaps between the resonator sections.

The spectral domain approach (SDA) is used for the analysis of the broadside-coupled microstrip lines to obtain the characteristic impedances and the dielectric constants of the propagation modes. Also the algorithm of the SDA is tested by applying it to the analysis of the coupled suspended microstrip line with tuning septums on the lower side of the suspended dielectric layer.

By the analysis of the broadside-coupled microstrip lines structure the relation between the PCL-BPF structure parameters and the characteristic impedances is obtained. Finally, Comparison between the two filter layouts for different fractional bandwidths will be presented, and the effect of the variation of the filter structure parameters on the filter response is studied.

LIST OF FIGURES

Figure		Page
Fig. 2.1	Cross section of shielded multiconductor printed line	9
Fig. 2.2	Cross section of coupled suspended microstrip lines with tuning septums	13
Fig. 2.3	Characteristic impedances of the coupled suspended lines versus the slit width, h= *1.64mm*, W/h=*1.2*, $L/h=b/h=t/h$=*10.0*, s/h=*0.2*, and ε_{r2}=*2.4*.	26
Fig. 2.4	Normalized guide wavelength of the coupled suspended lines versus the slit width, h=*1.64mm*, W/h=*1.2*, $L/h=b/h=t/h$=*10.0*, s/h=*0.2*, and ε_{r2}=*2.4*.	26
Fig. 3.1	Cross sections of the broadside-coupled microstrip line	28
Fig. 3.2	Even and odd-modes characteristic impedances versus 'W/L' of the structure shown in Fig. 3.1a, with d/L=*4*, h/L=*0.1*.	41
Fig. 3.3	C-mode and π-mode characteristic impedances and effective dielectric constants of the structure shown in Fig. 3.1a, versus W_2, with W_1=40mm.	43
Fig. 3.4	C-mode and π-mode parameters of the structure shown in Fig. 3.1b, versus the offset 'S', with $\varepsilon_{r1}=\varepsilon_{r2}$=1, ε_{r2}=10.5	44
Fig. 3.5	The mode characteristic impedances versus 'ε_{r2}' of the symmetrical structure shown in Fig. 3.1a, with $\varepsilon_{r1}=\varepsilon_{r3}$=1.	45
Fig. 3.6	The mode characteristic impedances versus 'h/d' of the symmetrical structure shown in Fig. 3.1a,	45
Fig. 4.1	Two-port network representation in terms of voltage and currents.	52
Fig. 4.2	Cascade of two-port networks.	53

Figure		Page
Fig. 4.3	Two-port network representation in terms of incident and reflected voltage waves.	55
Fig. 4.4	Network for defining image impedance	56
Fig. 4.5	Network for defining image transfer constant	57
Fig. 4.6	The process of filter design by the insertion loss method	58
Fig. 4.7	Low pass characteristic for the Butterworth and the Chebychev low pass characteristic	60
Fig. 4.8	Prototype ladder network for low pass filter.	61
Fig. 4.9	Transformation from low pass prototype to band pass filter	62
Fig. 4.10	Richard's Transformation.	64
Fig. 4.11	Kuroda's four identities ($n^2 = 1 + Y_a Z_b$)	65
Fig. 4.12	A parallel-coupled lines band pass filter	66
Fig. 4.13	One section of the parallel coupled lines band pass filter shown in Fig. 4.12	67
Fig. 4.14	Image impedance versus kl (real range) for the coupled lines section of Fig. 4.13. Identical coupling sections.	68
Fig. 4.15	Equivalent circuit for the single parallel-coupled lines section of Fig.4.13	69
Fig. 4.16	Equivalent circuit of multisection parallel coupled lines bandpass filter shown in Fig. 4.12.	71
Fig. 5.1	Implementation of the broadside PCL-BPF with open-end resonator sections for $N=3$	74

Figure		Page
Fig. 5.2	Implementation of the broad side PCL-BPF with gaps between the resonator sections for $N=3$.	75
Fig. 5.3	Calculated S_{12} and S_{11} of the PCL-BPF when varying Z_{en} for Chebychev and Butterworth response.	80
Fig. 5.4	Calculated S_{12} and S_{11} of the PCL-BPF when varying Z_{on} for Chebychev and Butterworth response.	82
Fig. 5.5	Calculated S_{12} and S_{11} of the PCL-BPF when varying Z_{en} and Z_{on} for Chebychev and Butterworth response.	84
Fig. 5.6	Calculated S_{12} and S_{11} of the PCL-BPF type 1 with and without including open-end capacitances $C_{o.e.}$ for Chebychev and Butterworth response	88
Fig. 5.7	Effect of varying the strip widths 'W_n' of the resonator structures on the response of the PCL-BPF type 1.	90
Fig. 5.8	Effect of varying the resonators section width 'L' on the response of the PCL-BPF type 1.	91
Fig. 5.9	Effect of varying the substrate dielectric constant 'ε_{r2}' of the resonator structures on the response of the PCL-BPF type 1.	92
Fig. 5.10	Effect of varying the substrate height 'h' of the resonator structures on the response of the PCL-BPF type 1.	93
Fig. 5.11	Effect of varying the height, 'd_n', of the resonator structure 'd_n' on the response of the PCL-BPF type 1.	94
Fig. 5.12	Calculated S_{12} and S_{11} of the PCL-BPF type 2, with different values of gaps widths for Chebychev and Butterworth response.	97
Fig. 5.13	Calculated S_{12} and S_{11} of the PCL-BPF type 2, with and without including gaps effect for Chebychev and Butterworth response.	99
Fig. 5.14	Effect of varying the strip widths 'W_n' of the resonator structures on the response of the PCL-BPF type 2.	101

Figure		Page
Fig. 5.15	Effect of varying the resonators section width 'L' on the response of the PCL-BPF type 2.	102
Fig. 5.16	Effect of varying the substrate dielectric constant 'ε_{r2}' of the resonator structures on the response of the PCL-BPF type 2.	103
Fig. 5.17	Effect of varying the substrate height 'h' of the resonator structures on the response of the PCL-BPF type 2.	104
Fig. 5.18	Effect of varying the height of the resonator structure 'd_n' on the response of the PCL-BPF type 2.	105
Fig. 5.19	Calculated S_{12} and S_{11} of the PCL-BPF's with different fractional bandwidths for Chebychev response.	109
Fig. 5.20	Calculated S_{12} and S_{11} of the PCL-BPF's with different fractional bandwidths for Butterworth response.	111
Fig. 5.21	The sensitivity of the response of the PCL-BPF's to the resonator structure parameters	113
Fig. B.1	Microstrip Open End Discontinuity, and its equivalents.	121
Fig. B.2	A Microstrip Gap and its Equivalent circuit	122
Fig. C.1	Transmission line and development of its equivalent circuit.	125
Fig. C.2	Equivalent circuit of multisection parallel coupled lines band pass filter and its lumped element counterpart.	126
Fig. C.3	Equivalent of an admittance inverter and an ideal transformer plus $\lambda/4$ line section.	127
Fig D.1	Equivalent circuits for the gap in microstrip with unequal widths	133

LIST OF TABLES

Table		Page
Table (2.1)	The even- and the odd-mode characteristic impedances for different choice of basis functions	24
Table (3.1)	Characteristic impedances and effective dielectric constants of the symmetrical broadside-coupled microstrip line, of Fig. 3.1a; with $W_1=W_2=W$, $S=0.0$ *mm*, $t=b$, $L=180$ *mm*, $\varepsilon_{r1}=\varepsilon_{r3}=1$ *and* $\varepsilon_{r2}=2.5$.	46
Table (4.1)	Transmission matrix parameters of some basic circuit elements	54
Table (5.1)	Parameters of the PCL-BPF for Chebychev response with different bandwidths.	77
Table (5.2)	Parameters of the PCL-BPF for Butterworth response with different bandwidths.	78
Table (5.3)	Coupling factor for each section of the PCL-BPF with Chebychev and Butterworth response	79
Table (5.4)	The parameters, l_n and Δl_n of PCL-BPF type 1, For Chebychev and Butterworth response with $\Delta\omega = 12\%$.	87
Table (5.5)	The parameters $G_{n,n+1}$, l_n and Δl_n of the PCL-BPF type 2, with $\Delta\omega = 12\%$	96
Table (5.6)	The parameters, l_n and Δl_n of PCL-BPF type 1, with different bandwidths for Chebychev and Butterworth response.	106
Table (5.7)	The parameters $G_{n,n-1}$, l_n and Δl_n of PCL-BPF type 2, with different bandwidths for Chebychev and Butterworth response.	107
Table (B.1)	Coefficients C_i that appear in the empirical equation (B.1)	121